

Fabrication and investigation of organic-inorganic semitransparent thermoelectric cells based on the composites of silicone-adhesive with Bi₂Te₃, graphene and carbon nanotubes

M. T. S. CHANI^{a,b,*}, KH. S. KARIMOV^{c,d}, JAMEEL-UN NABI^c, A. AHMED^c, I. KIRAN^c, A. M. ASIRI^{a,b}

^aCenter of Excellence for Advanced Materials Research, King Abdulaziz University, Jeddah 21589, P.O. Box 80203, Saudi Arabia

^bChemistry Department, Faculty of Science, King Abdulaziz University, Jeddah 21589, P.O. Box 80203, Saudi Arabia

^cGhulam Ishaq Khan Institute of Engineering Sciences and Technology, Topi-23640, District Swabi, KPK, Pakistan

^dCenter for Innovative Development of Science and New Technologies of Academy of Sciences of Tajikistan, Dushanbe, 734025, Rudaki 33, Tajikistan

This work describes the fabrication and investigation of semitransparent thermoelectric cells based on composites of p-type bismuth telluride (p-Bi₂Te₃), n-type bismuth telluride (n-Bi₂Te₃), p-Bi₂Te₃-CNTs, n-Bi₂Te₃-CNTs, graphene and CNTs with silicone adhesive. Cells were fabricated by the screen printing of composites. Technology used for cells fabrication would be acceptable for organic and inorganic materials, especially for low power applications. Electric and thermoelectric parameters; resistance and Seebeck coefficient of the samples were investigated in temperature range of 27-75 °C. Transparency of the samples was measured, which was in the range of 49-65%. The maximum value of Seebeck coefficient was observed at 335K which was 210 (μV/K) for P-Type and -190 (μV/K) for N-Type Bi₂Te₃, respectively. The Figure of merit (ZT) of all the samples was calculated and was up to 0.95 at 335 K.

(Received December 12, 2018; accepted October 9, 2019)

Keywords: Organic and inorganic material, Screen printing, Seebeck coefficient, Figure of merit, Transparency

1. Introduction

The investigation of semitransparent solar cell's structure, properties and characteristic shows that semitransparent cells are less efficient as compared to opaque cells and their fabrication is complex because of thin films deposition. So, the thermoelectric-cells and generators (TEGs) are the alternative approach, which are simple in structure due to lack of Schottky or p-n junctions and multilayers [1, 2]. As for as efficiency is concerned recently p-type compound (MgAgSb) based thermoelectric-leg showed 8.5% efficiency in 20 to 245 °C temperature range [3]. By raising hot side's temperature up to 295 °C the 10% increase in efficiency may achieved that is comparable to solar cell's efficiency. To eliminate the conventional metallization process the one-step hot-press technique was used for silver contact pads deposition. By this the simplified manufacturing of thermoelectric elements with low contact resistances (thermal and electrical) becomes viable.

A bulk silicon based semi-transparent flexible thermoelectric energy harvester was fabricated by growing 300 nm silicon oxide film followed by deposition of Bi₂Te₃ (n-type) and Sb₂Te₃ (p-type) thin films [4]. At 314 K the Seebeck coefficients were -37μV/K and 340 μV/K for Bi₂Te₃ and Sb₂Te₃, respectively. The resistivity of Bi₂Te₃ and Sb₂Te₃ was 2.22 μΩ·m and 638 μΩ·m, accordingly at 304 K, while the

power factor was 0.6 mW/K² and 9.02 x 10⁻² for Bi₂Te₃ and Sb₂Te₃, respectively.

A thermal model was derived for the semi-transparent photovoltaic thermal with thermoelectric collector (PVT-TEC), which was based on total energy balance maintained by PVT-TEC's components [5]. By comparing the efficiency of the PVT-TEC collector with Semi-transparent photovoltaic (PV) and semitransparent photovoltaic thermoelectric (PV-TEC) collectors it was found that PVT-TEC was 7.266% and 4.723% more efficient than PV and PV-TEC collectors, respectively.

The efficiency (Z) of the thermoelectric cells is determined by the following relationship that was derived by Ioffe [6]:

$$Z = \frac{\sigma \alpha^2}{k} \quad (1)$$

where, σ is the electrical conductivity, k is the thermal conductivity, and α is the Seebeck coefficient. Afterward the ZT a dimensionless-figure of merit was introduced as well [7] that is the product of average temperature (\bar{T}) and Z.

$$\bar{T} = \frac{T_1 + T_2}{2} \quad (2)$$

where T_1 and T_2 are temperatures of two contacts.

Depending upon some conditions the higher ZT causes higher efficiency especially when the two materials of the couple have similar Z values. The ZT is thought to be a method by which the potential thermoelectric efficiencies of the devices can be compared using various materials. The 1 is thought good value for ZT ; but for efficiency competition with mechanical devices the ZT values from 3 to 4 are important. So far, the ZT highest reported value is ~ 2 [8, 9]. The reduction in k and increase in Seebeck coefficient (α) through nanostructure manipulation is the prime focus of thermoelectric material's research.

Following expression is used to determine the Maximum energy efficiency:

$$\eta_{max} = \left(\frac{T_H - T_C}{T_H} \right) \left(\frac{\sqrt{1 + Z\bar{T}} - 1}{\sqrt{1 + Z\bar{T}} + (T_C/T_H)} \right) \quad (3)$$

where, T_H and T_C are the temperature at hot junction and cold surface, correspondingly, while the $Z\bar{T}$ is modified dimension-less figure of merit, which reflects thermoelectric-capacity of the device's materials (both materials). The $Z\bar{T}$ is presented as

$$Z\bar{T} = \frac{(\alpha_p - \alpha_n)^2 \bar{T}}{[(\rho_n k_n)^{1/2} + (\rho_p k_p)^{1/2}]^2} \quad (4)$$

where, ρ and \bar{T} and the electrical resistivity and the average temperature (b/w cold and hot surfaces), respectively. The p and n subscripts specifying the characteristics related to semiconducting p and n type thermoelectric materials, correspondingly.

For the fabrication of the thermoelectric generators different methods and technologies are used [10-17] depending upon the material's type and technology. In this paper we have used the screen printing technology for the thermoelectric cells fabrication which would be acceptable for organic and inorganic materials, especially for low power applications.

Taking into account the potential advantages of the semitransparent power generating devices, i.e. solar cells, according to the best our knowledge in this paper we are presenting first time the design, fabrication, investigation and properties of the semitransparent thermoelectric cells based on the composites of Bi_2Te_3 , graphene and CNTs with silicone adhesive.

2. Experimental

For fabrication of the thermoelectric cells the following materials were purchased from Sigma Aldrich: powders of the p- Bi_2Te_3 , n- Bi_2Te_3 , graphene, CNTs and silicone adhesive. For the fabrication of thermoelectric cells following technology was used: the thermoelectric materials (organic or inorganic) were mixed with the same silicone adhesive in order to make the composites. The samples were fabricated by screen printing technology using the composites of the thermoelectric materials. This technology of thermoelectric cells fabrication would be acceptable especially for the demonstrative purposes and low power applications. The basic thermoelectric properties i.e. Seebeck coefficient, figure of merit (ZT) and efficiency were estimated and compared for all the cells. Fig. 1 shows the schematic diagrams of the graphene and CNTs. Thermoelectric cells were fabricated by the following way: the powders of the p- Bi_2Te_3 , n- Bi_2Te_3 , graphene and CNTs were separately mixed with equal weight of silicone adhesive and deposited by screen printing on glass substrate at $T = 25^\circ\text{C}$. For the p- Bi_2Te_3 -CNTs, n- Bi_2Te_3 -CNTs samples the concentration of the ingredients were the following: 25wt. % (p- Bi_2Te_3 or n- Bi_2Te_3), 25wt. % (CNTs) and 50wt. % of the silicone adhesive. As a result six group of samples were fabricated: p- Bi_2Te_3 , n- Bi_2Te_3 , p- Bi_2Te_3 -CNTs, n- Bi_2Te_3 -CNTs, graphene and CNTs with silicone adhesive. The average sizes of the strips in the samples were equal to $10 \times 4 \times 0.1 \text{ mm}^3$. The gap between two strips was equal to 4mm. The samples structures of thermoelectric cells are shown in Fig. 2: it is actually like to grid structure.

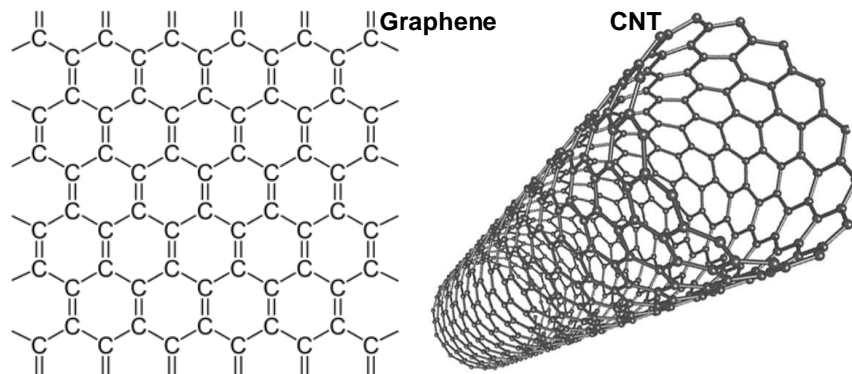


Fig. 1. Schematic diagrams of the two-dimensional graphene[18] and the carbon nanotubes (CNTs) [19]

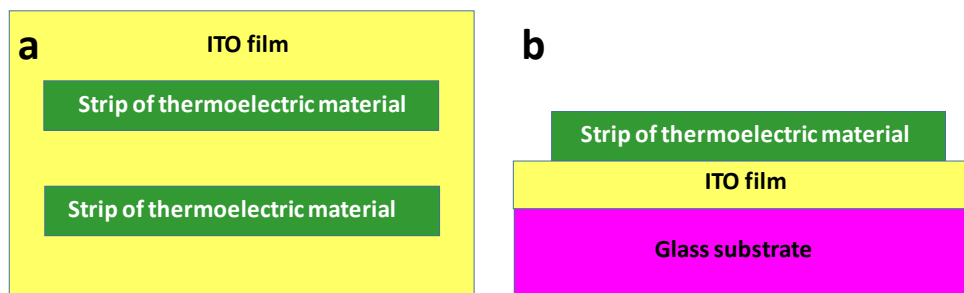


Fig. 2. The schematic diagrams of the top view (a) and front view (b) of the thermoelectric cells

The transparency for each thermoelectric cell was measured experimentally by using the Illuminometer and the filament lamp as a light source and it was found in the range of 49 to 65 % (Fig.3). The transparency also depends on the ratio of areas covered by the thermoelectric materials strips and uncovered glass substrate. Recently, thermoelectric properties of the graphene/ Cu_2SnSe_3 composite [20], graphene oxide patterned by nanorods [21] and graphene/ MoS_2 /graphene hetero-structure [22] were investigated and it was shown that ZT of graphene can be improved through the fabrication of complex material or by growing the special structures. But these thermoelectric cells were opaque, not semitransparent.

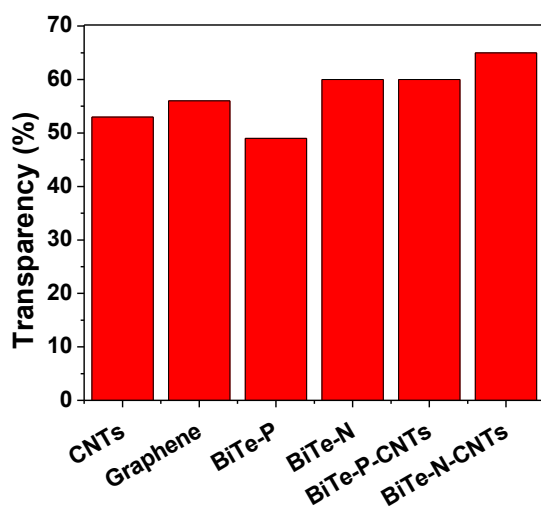


Fig. 3. Transparency of the CNTs, grapheme, $p\text{-Bi}_2\text{Te}_3$, $n\text{-Bi}_2\text{Te}_3$, $p\text{-Bi}_2\text{Te}_3\text{-CNTs}$ and $p\text{-Bi}_2\text{Te}_3\text{-CNTs}$ composite samples

The differences of temperatures (8°C) in horizontal direction (along the glass substrate plane in Fig.2) of two sides of the samples were created by use of small electric heaters and were measured by FLUKE 87. The voltages generated due to the thermoelectric effect in the samples were measured by HIOKI DT 4252, while the light intensity was measured by illuminometer LM-80.

3. Results and discussions

The Fig. 4 (a-f) shows the dependence of the resistances of the composite samples on the temperature. It is also evident from the Fig. (Fig.4 (a-f)) that the resistance-temperature relationships for the CNTs and graphene have “metallic” behavior: as the temperature increases the resistance also increases: it may be due to the decrease of the mobility of charges as in the metals. On the other hand the resistance-temperature dependences for all Bi_2Te_3 samples, including the samples containing CNTs, are like to semiconductors: as the temperature increases the resistance decreases. This behavior may be credited to the increasing concentration of charge carriers with increase in temperature due to the presence of energy gap in the semiconductors.

Actually investigations of the thermoelectric power and conductivity in the extrinsic range of pure Bi_2Te_3 indicated that the samples were degenerate [23]. Temperature dependence of mobility was $T^{-1.63}$ for electrons and $T^{-1.94}$ for holes. In the high temperature by measurement of the conductivity it was found that the energy gap was 0.21 eV. The Hall coefficient in the extrinsic range is anomalous and the explanation is not known. Though we investigated the properties of the composite it can be considered that there are some similarities in their properties with pure Bi_2Te_3 .

The Fig. 5 (a-f) shows the dependence of the Seebeck coefficients of the composite samples on the temperature. It can be seen from the Fig.5 (a-f) that the Seebeck coefficient for all the samples is almost increasing up to $T=345\text{K}$. But only for the $p\text{-Bi}_2\text{Te}_3$ and $n\text{-Bi}_2\text{Te}_3$ samples the saturation and the maximum value of Seebeck coefficient were observed at 335K. The typical Seebeck coefficient values are 210 ($\mu\text{V}/\text{K}$) for P-Type and -190 ($\mu\text{V}/\text{K}$) for N-Type Bi_2Te_3 , respectively. The Seebeck coefficient behavior is consistency with previous studies [24]. Moreover, the voltage was increasing linearly with temperature gradient of up to 50°C . In the first approximation the Seebeck coefficient and temperature relationships shown in Fig.5 can be explained by the following approach; in the absence of the energy gap (as in metals) the increase in temperature caused to increase the Seebeck coefficient because the concentration of charge carriers does not increase. But in the presence of energy gap (as in semiconductors) the thermoelectric coefficient decreases with increase in temperature due to increase in the concentration of the charge carriers. It is evident from

Fig. 5 and Table 1 that the electrical conductivity, Seebeck coefficient and Figure of merit decreased in the p-Bi₂Te₃-CNTs and n-Bi₂Te₃-CNTs composites as compared to pure p-Bi₂Te₃ and n-Bi₂Te₃, which may be credited to the hindrance in the carrier mobility [25].

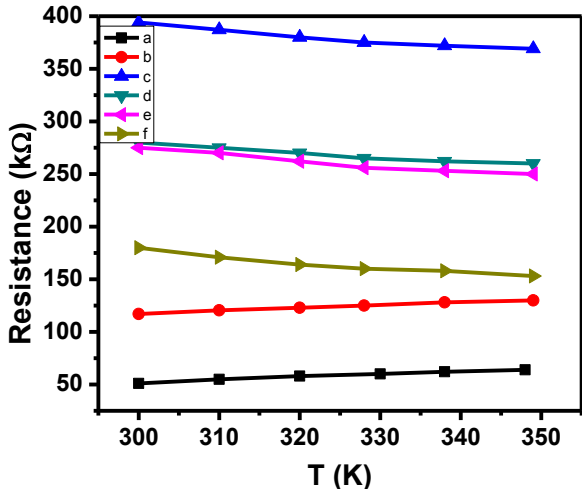


Fig. 4. Resistance-temperature relationships for the composites of adhesive with: CNTs (a), graphene (b), p-Bi₂Te₃(c), n-Bi₂Te₃ (d), p-Bi₂Te₃-CNTs (e), n- Bi₂Te₃-CNTs (f)

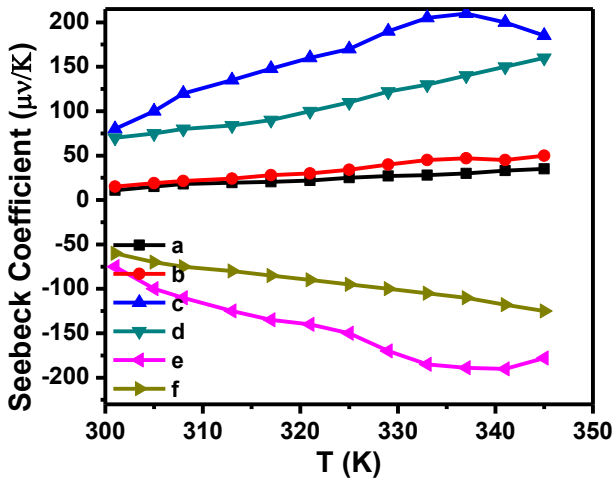


Fig. 5. Seebeck coefficient and temperature (T) relationships for the composites of adhesive with: CNTs (a), graphene (b), p-Bi₂Te₃ (c), p-Bi₂Te₃-CNTs(d), n- Bi₂Te₃(e) and n-Bi₂Te₃-CNTs (f)

For the estimation of the figure of merit and efficiency the electrical conductivity (Eq. 1) was calculated from the measured resistances of the samples. In the first approximation the following values of the thermal conductivity were used for the calculations of ZT [26-32]: 2.4-2.2 W/mk (p-Bi₂Te₃), 2.5-2.4 W/mk (n-Bi₂Te₃), 50 W/mk (CNTs) and 50W/mk (graphene). For the mixed combination of the materials the average values of the thermal conductivities of the components were taken as 26 W/mk (p-Bi₂Te₃+CNTs) and 20 W/mk (n-Bi₂Te₃+CNTs). By using the values of experimentally obtained Seebeck

coefficient and the thermal conductivity (obtained from references [26-32]) the figure of merit and the efficiency was calculated.

Fig. 6 shows the dependence of the figure of merits on temperature for the composites of adhesive with CNTs, graphene, p-Bi₂Te₃, n-Bi₂Te₃, p-Bi₂Te₃-CNTs, and n-Bi₂Te₃-CNTs. It is evident from the figure (Fig.6) that the p-Bi₂Te₃ exhibits a highest Figure of merit as compared to other tested materials.

The increase in efficiency (Z) and figure of merit (ZT) [7] with increase in temperature may be considered not only due to the increase in conductivity and Seebeck coefficient but also due to the decrease in thermal conductivity (Eq.1). In Table-1 the summary of various thermoelectric parameters of the fabricated cells is presented.

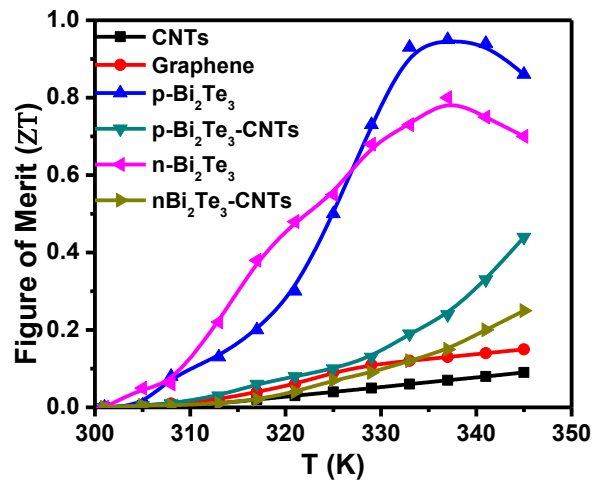


Fig. 6. Figure of merit (ZT) and temperature (T) relationships for the samples of composites of adhesive with CNTs, graphene, p-Bi₂Te₃, n-Bi₂Te₃, p-Bi₂Te₃-CNTs, and n-Bi₂Te₃-CNTs

Table 1. Summary of various thermoelectric parameters of the fabricated cells

Sample	α ($\mu\text{V/K}$)	ZT	η (% age)
CNTs	35	0.08	0.25
Graphene	50	0.15	0.5
p-Bi ₂ Te ₃	210	0.95	2.5
n-Bi ₂ Te ₃	-190	0.8	2.2
p-Bi ₂ Te ₃ -CNTs	152	0.44	1.4
n- Bi ₂ Te ₃ -CNTs	-120	0.26	0.9

The Seebeck coefficient usually increases with temperature in a number of metals [33]. On the contrary in general the thermoelectric coefficient of the semiconductors decreases with increase in temperature, but the actual behavior depends upon the kind and concentration of semiconductor's impurities [33]. The Seebeck coefficient of the metals is determined by the following expression [34]:

$$\alpha \approx C_{el}/q \approx (k_B/e) (k_B T/E_F) \quad (5)$$

Accordingly for the Seebeck coefficient of semiconductors is the following:

$$\alpha \approx C_{el}/q \approx (k_B/e) (E_g/k_B T) \quad (6)$$

It is evident from Fig. 5 that thermoelectric cells based on composites of adhesive with CNTs, graphene and p-Bi₂Te₃ follow the Eq.6 i.e. showing semiconductive behavior (Fig.5 a, b, c and e), while the thermoelectric cells based on composites of adhesive with n-Bi₂Te₃ and n-Bi₂Te₃-CNTs follow the Eq.5 i.e. showing the metallic behavior (Fig.5 d and f). In fact the n- Bi₂Te₃ and n-Bi₂Te₃-CNTs seem to have complex thermoelectric properties. So, in the case of complex semiconductors that demonstrate hole conduction (positive thermo-power) or electron conduction (negative thermo-power) or both together the weighted average of their electrical conductivities (σ_n and σ_p) is used to calculate the thermo-power (α) [34]:

$$\alpha \approx (\alpha_n \sigma_n + \alpha_p \sigma_p) / (\sigma_n + \sigma_p) \quad (7)$$

By using these results a semitransparent thermoelectric cells can be developed, especially the cells for solar energy conversion. Our initial studies showed that for the development of semitransparent solar thermoelectric cells the plane cells may be used as a prototype: the transparent conductive glass substrates covered by ITO, which have three major parts: plane semitransparent part, the plane collector and the plane reflector that are located in opposite position on two sides of semitransparent part. The prototype of the simplified semitransparent thermoelectric cells is illustrated in Fig.7. As the light reflects from reflector and absorbed by the collector the temperature gradient is developed which causes to generate voltage.

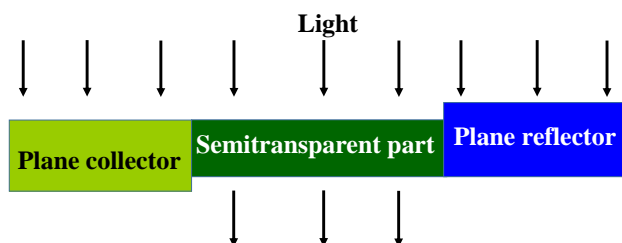


Fig. 7. Simplified prototype of the semitransparent solar thermoelectric cell

4. Conclusion

The semitransparent thermoelectric cells based on p-Bi₂Te₃, n-Bi₂Te₃, p-Bi₂Te₃-CNTs, n-Bi₂Te₃-CNTs, graphene and CNTs with silicone adhesive were fabricated and investigated. The sufficiently high values of Seebeck coefficients and ZT were observed in the case of n-Bi₂Te₃ and p-Bi₂Te₃ composites with silicone adhesive. The fabricated thermoelectric devices showed good response to

the temperature in the range from 27 °C to 75°C. Moreover, the voltage was increasing linearly with the temperature gradient. The transparency was experimentally observed for each of the thermoelectric materials devices. Semitransparent thermoelectric cells and generators can have a visible contribution in the field of thermoelectricity. On the base of the obtained results a simplified prototype of the semitransparent solar thermoelectric cell was developed for the conversion of solar energy into electric energy. In any case the main and most important practical target is to increase the ZT by physical, technological or chemical way or their combinations. It can be considered that this area of power technology will be developed in coming future that allows to use it wider in practice [35-38].

Commercial thermoelectric materials have ZT~ 1 and accordingly low energy conversion efficiency (~5%). If thermal conductivity of the material can be decreased the ZT value would be greater, for example, than 3 and accordingly efficiency of the thermoelectric cells can be increased as well [39]. Future development of the theoretical approaches and experiments in the area of materials sciences will show whether nanomaterials based thermoelectric generators will be economically acceptable for practical applications in the wide scale or not.

In [40, 41] the progress in thermoelectric materials, including traditional semiconductors and conjugated polymers as well were described in detail. In [4] it was described flexible and semitransparent thermoelectric energy harvesters from low cost bulk silicon (100). The use of the theoretical approaches for calculation and explanation of the obtained (by us) results definitely will be the matter of our future research work. We would like to emphasize that the temperature range covered by our experiments was limited by our experimental facilities.

Acknowledgements

This project was funded by the Deanship of Scientific Research (DSR) at King Abdulaziz University, under grant no. G-1501-130-40. The authors, therefore, acknowledge with thanks DSR for technical and financial support.

References

- [1] K. S. Karimov, Energy Science and Technology **6**, 302 (2015).
- [2] K. S. Karimov, M. Abid, K. Y. Cheong, M. M. Bashir, in Two-dimensional nanostructures for energy-related applications (K. Y. Cheong, ed.), Taylor & Francis Group, Boca Raton, London, New York, p. 48, 2016.
- [3] D. Kraemer, J. Sui, K. McEnaney, H. Zhao, Q. Jie, Z. F. Ren, G. Chen, Energy Environ. Sci. **8**, 1299 (2015).
- [4] G. A. T. Sevilla, S. B. Inayat, J. P. Rojas, A. M. Hussain, M. M. Hussain, Small **9**, 3916 (2013).

- [5] N. Dimri, A. Tiwari, G. N. Tiwari, *Energy Convers. Manage.* **146**, 68 (2017).
- [6] A. Ioffe, Infosearch, Ltd., London, 1957.
- [7] A. Bulusu, D. G. Walker, *Superlattices and Microstructures* **44**, 1 (2008).
- [8] K. Biswas, J. He, I. D. Blum, C.-I. Wu, T. P. Hogan, D. N. Seidman, V. P. Dravid, M. G. Kanatzidis, *Nat.* **489**, 414 (2012).
- [9] K. F. Hsu, S. Loo, F. Guo, W. Chen, J. S. Dyck, C. Uher, T. Hogan, E. Polychroniadis, M. G. Kanatzidis, *Sci.* **303**, 818 (2004).
- [10] I. Matsubara, R. Funahashi, T. Takeuchi, S. Sodeoka, T. Shimizu, K. Ueno, *Appl. Phys. Lett.* **78**, 3627 (2001).
- [11] M.-Z. Yang, C.-C. Wu, C.-L. Dai, W.-J. Tsai, *Sens.* **13**, 2359 (2013).
- [12] M. Chani, H. Marwani, E. Danish, K. S. Karimov, M. Hilal, A. Hagfeldt, A. Asiri, *J. Optoelectron. Adv. M.* **19**(3-4), 178 (2017).
- [13] M. T. S. Chani, A. M. Asiri, K. S. Karimov, M. Bashir, S. B. Khan, M. M. Rahman, *Int. J. Electrochem. Sci.* **10**, 3784 (2015).
- [14] M. T. S. Chani, K. S. Karimov, A. M. Asiri, N. Ahmed, M. M. Bashir, S. B. Khan, M. A. Rub, N. Azum, *PLoS ONE* **9**, e95287 (2014).
- [15] M. T. S. Chani, K. S. Karimov, S. B. Khan, A. M. Asiri, *Int. J. Electrochem. Sci.* **10**, 5694 (2015).
- [16] M. T. S. Chani, K. S. Karimov, J.-u. Nabi, M. Hashim, I. Kiran, A. M. Asiri, *Int. J. Electrochem. Sci.* **13**, 11777 (2018).
- [17] M. T. S. Chani, S. B. Khan, A. M. Asiri, K. S. Karimov, M. A. Rub, *J. Taiwan Inst. Chem. Eng.* **52**, 93 (2015).
- [18] <http://www.quirkyscience.com/graphene-properties/>,
- [19] <https://warosu.org/sci/thread/6873365>.
- [20] D. Zhao, X. Wang, D. Wu, *Cryst.* **7**, 71 (2017).
- [21] S. Zhou, Y. Guo, and J. Zhao, *Phys. Chem. Chem. Phys.* **18**, 10607 (2016).
- [22] H. Sadeghi, S. Sangtarash, C. J. Lambert, *2D Mater.* **4**, 015012 (2016).
- [23] R. Mansfield, W. Williams, *Proc. Phys. Soc.* **72**, 733 (1958).
- [24] H. Goldsmid, in *Proceedings ICT'06. 25th International Conference on Thermoelectrics*, Vienna, IEEE, p. 5 (2006).
- [25] E. Voroshazi, M. B. Yaala, G. Uytterhoeven, J. G. Tait, R. H. Andriessen, Y. Galagan, D. Cheyns, in *Photovoltaic Specialist Conference (PVSC)*, IEEE 42nd, New Orleans, LA, USA, p. 1 (2015).
- [26] H. Goldsmid, *Mater.* **7**, 2577 (2014).
- [27] R. Bude, L. Divay, R. Bisaro, B. Servet, E. Leveugle, F. Wyczisk, D. Carisetti, A. Ziaei, S. Volz, in *21st International Workshop on Thermal Investigations of ICs and Systems (THERMINIC)*, IEEE, p. 1 (2015).
- [28] T. Suriwong, T. Plirdpring, T. Threrujirapong, T. Thongtem, S. Thongtem, *Micro Nano Lett.* **10**, 19 (2015).
- [29] J. Che, T. Cagin, W. A. Goddard III, *Nanotechnol.* **11**, 65 (2000).
- [30] P. Jiang, H. Liu, D. Fan, L. Cheng, J. Wei, J. Zhang, J. Liang, J. Shi, *Phys. Chem. Chem. Phys.* **17**, 27558 (2015).
- [31] A. A. Balandin, arXiv preprint arXiv:1106.3789, (2011).
- [32] D. Hayashi, T. Ueda, Y. Nakai, H. Kyakuno, Y. Miyata, T. Yamamoto, T. Saito, K. Hata, Y. Maniwa, *Appl. Phys. Express* **9**, 025102 (2016).
- [33] M. A. Batal, G. Nashed, F. H. Jneed, *J. Assoc. Arab Uni. Basic Appl. Sci.* **15**, 15 (2014).
- [34] J. Terada, T. Nitta, Vol. US4378691A, U.S Patent, U. S, 1983.
- [35] C. L. Izidoro, O. H. Ando Junior, J. P. Carmo, L. Schaeffer, *Meas.* **106**, 283 (2017).
- [36] J. P. Carmo, J. Antunes, M. F. Silva, J. F. Ribeiro, L. M. Goncalves, J. H. Correia, *Measurement* **44**, 2194 (2011).
- [37] O. Ando Junior, J. Ferro, C. Izidoro, E. Maestrelli, A. Spacek, J. Mota, C. Malfatti, *Renewable Energy Power Qual. J.* **1**, 227 (2014).
- [38] L. Xu, Y. Xiong, A. Mei, Y. Hu, Y. Rong, Y. Zhou, B. Hu, H. Han, *Adv. Energy Mater.* **8**, 1702937 (2018).
- [39] Z.-G. Chen, G. Han, L. Yang, L. Cheng, J. Zou, *Prog. Nat. Sci.: Mater. Int.* **22**, 535 (2012).
- [40] C.-J. Yao, H.-L. Zhang, Q. Zhang, *Polym.* **11**, 107 (2019).
- [41] J.-C. Zheng, *Front. Phys. China* **3**, 269 (2008).

*Corresponding author: tariqchani1@gmail.com
mtmohamad@kau.edu.sa